PROCEEDINGS, TOUGH Symposium 2012
Lawrence Berkeley National Laboratory, Berkeley, California, September 17-19, 2012

# NUMERICAL MODELING OF GEOTHERMAL SYSTEMS: THE EFFECT OF OVERPRESSURE AND INJECTION FLUID TEMPERATURE IN INDUCING MICROEARTHQUAKES, WITH APPLICATION TO A NEW ZEALAND GEOTHERMAL FIELD

Lauriane Chardot[1,2], Steven Sherburn[1], Nicolas Fournier[1]

[1]GNS Science – Wairakei Research Centre
114 Karetoto Road, SH1, Wairakei
Taupo, 3377, New Zealand
e-mail: l.chardot@gns.cri.nz

[2]EOST, Strasbourg, France (now at University of Canterbury, Christchurch, New Zealand and GNS Science)

## ABSTRACT

Induced seismicity in active geothermal areas is often thought to be linked to the re-injection of cold fluids into the subsurface hot rock which is close to failure. However, fluid flow processes leading to failure are poorly understood, because they are intrinsically complex and interrelated. Using a numerical modeling approach, this study aims at a better understanding of how overpressure and injection fluid temperature could potentially induce microearthquakes. Multiphase fluid flow in a homogeneous porous medium and the poroelastic and thermal response of this medium were modeled using the TOUGH2/BIOT2 package. The model was based on characteristics representative of a geothermal field located in the Taupo Volcanic Zone, New Zealand, but does not include pre-existing fractures. Stresses were computed over time, with a Mohr-Coulomb failure criterion defined to assess when and where failure (microearthquakes) was most likely to occur. A range of simulations were run to characterize the driving process for failure (poroelastic versus thermal). Finally, a sensitivity analysis to key parameters highlights the paramount importance of injection parameters and of the reservoir *in situ* properties on the occurrence and location of induced seismicity.

## INTRODUCTION

Induced seismicity has often been linked to geothermal activity when some fluid is injected into—or extracted from the subsurface hot rock (Majer et al., 2007). Indeed, if some areas are very close to failure, even a small change in the local stress field can lead to fracturing. However, the driving processes for induced seismicity remain poorly understood, because they are often interrelated, and any attempt at modeling them requires multiphysics numerical modeling strategies.

The aim of this study is to model the effect of two possible driving processes for microearthquakes: (1) the overpressure due to the injection of new fluid, and (2) the thermal effect due to the injection of cold fluids into a hot surrounding host rock. What is their respective role in the evolution of the stresses during the injection? Do they act at the same spacio-temporal scale? How do they affect the failure process?

We first describe our model, which is generic, but representative of a New Zealand geothermal field, along with our modeling approach (fluid flow simulation, stress computation and failure definition). We then present some general results about the evolution of stresses through time and the respective contribution of poroelasticity and thermoelasticity, along with their impact on the failure process. Finally, we show the effect of key parameters (cohesion, friction angle, shear modulus, thermal expansivity coefficient, injection rate, temperature of the injected fluid) on our modeling results, and discuss how failure could potentially be minimized.

## METHODOLOGY

### Model description

The model used in this study aims at being representative of conditions that can be encountered at the Rotokawa Geothermal Field, in the Taupo Volcanic Zone (TVZ), where local induced seismicity has been recorded following the commencement of deep fluid re-injection. Our geothermal field is considered to be quasi-circular in map view with a radius of 5 km. Fluids colder than the surrounding rock are injected through a well having a main feed zone at 2 km depth and situated at the center of the field.

Our representative model is 2D axi-symmetrical having a thickness of 2 km and a radius of 5 km (Figure 1), with its left edge representing the central axis of the geothermal field.

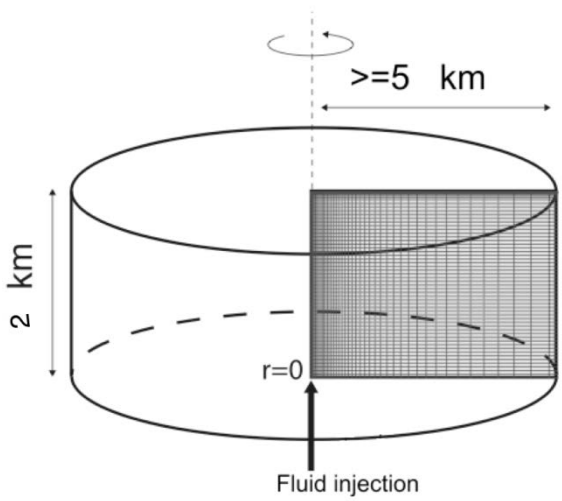


Figure 1. Computational domain for TOUGH2/BIOT2 simulations (adapted from Hutnak et al. (2009)).

The model is based on the work by Hutnak et al. (2009) on caldera-related processes, but modified to better fit the characteristics of the studied geothermal system: we use the same boundary conditions, but our model is smaller and has different input parameters. The host rock is considered to be homogeneous, with permeability and elastic parameters constant over the domain and through time. While our model remains simple, domain and input parameters are based on data from the Rotokawa geothermal field (temperature, porosity, permeability).

Fluids ($H_20$ and $CO_2$) at a temperature of 150°C are continuously injected into the host rock from a point source situated at the bottom-left corner of the half-domain, where the medium temperature is 300°C. The temperature of the injected fluids is specified using their respective enthalpy. Medium properties are adjusted to be representative of the Rotokawa Geothermal Field. However, we used a homogeneous permeability representative of the matrix—a mean value of the range of matrix permeabilities presented in Bowyer and Holt (2010), which is a lower limit of this parameter if the geothermal field contains fractures and if the fluid flow is fracture-controlled. The parameters used for our reference geothermal model are summarized in Table 1.

Table 1. Input parameters for TOUGH2/BIOT2 simulations.

| Parameter | Simulation values |
|---|---|
| Rock grain density | 2700 kg $m^{-2}$ |
| Porosity | 0.1 |
| Thermal conductivity | 2.8 W m-1 $°C^{-1}$ |
| Rock permeability | 1.2 mD |
| Rock grain specific heat | 1000 J $kg^{-1}$ $°C^{-1}$ |
| Basal heat flux | 400 mW $m^{-2}$ |
| $H_20$ injection rate | 97 kg $s^{-1}$ |
| Specific enthalpy of $H_20$ | $6.44\times10^5$ J $kg^{-1}$ |
| $CO_2$ injection rate | $10^{-12}$ kg $s^{-1}$ |
| Specific enthalpy of $CO_2$ | $5.23\times10^5$ J $kg^{-1}$ |
| Medium shear modulus | 8 GPa |
| Medium Poisson ratio | 0.25 |
| Medium thermal expansivity | $10^{-5}$ $°C^{-1}$ |
| Biot-Willis coefficient | 1 |

### Fluid flow modeling, stress computation and failure criterion definition

Majer et al. (2007) emphasized that processes leading to induced seismicity are complex and require coupled models. We therefore used the TOUGH2/BIOT2 modeling package—see Hurwitz et al. (2007) for details on the one-way coupling between TOUGH2 (Pruess, 1999) and BIOT2 (Hsieh, 1996)—in order to simulate fluid flow and associated deformation. This modeling package solves the following equation (Equation (1)):

$$G\nabla^2 u + \frac{G}{1-2\nu}\nabla(\nabla.u) - \nabla(p-p_0) - \frac{2G(1+\nu)\alpha}{3(1-2\nu)}\nabla(T-T_0) = 0 \quad (1)$$

where u is the displacement, G the shear modulus, ν the Poisson ratio, p the pore pressure, T the temperature, and α the thermal expansivity coefficient of the porous matrix. The simulation was run for 10 years to study the different time-scale processes. Outputs were extracted at 100 specific times and comprised the radial distance from the center of the domain and depth of each node, as well as the temperature and pressure at the center of each cell (Figure 2).

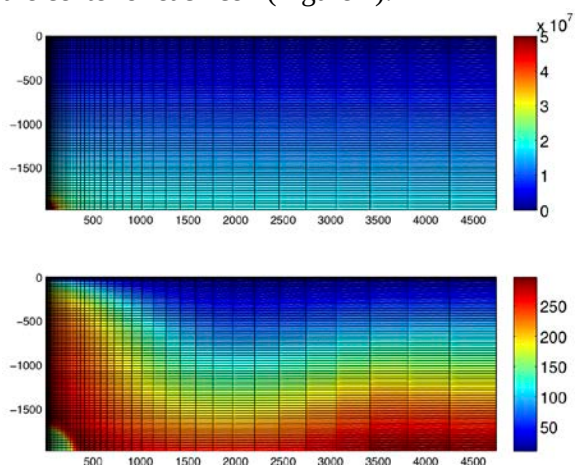


Figure 2. Pressure (Pa) (upper panel) and temperature (℃) (lower panel) within the domain (axes in meters) after 10 years of continuous injection.

We then followed the same procedure as Hsieh (unpublished) to compute strains and effective stresses from the displacement of each cell corner—Equations (2) and (3)—from which principal effective stresses are calculated. Positive normal stress is positive and positive normal strain denotes a shortening of length.

$$\epsilon_{ij} = -\frac{1}{2}(u_{i,j} + u_{j,i}) \quad (2)$$

$$\sigma_{ij}^{eff} = 2G\epsilon_{ij} + \frac{2\nu G}{1-2\nu}\epsilon\delta_{ij} \quad (3)$$

Finally, to assess when and where failure is most likely to occur during the simulation, we defined a Mohr-Coulomb criterion as in Jaeger et al. (2007) (Equation (4)), which forecasts failure if the condition below is true:

$$|\tau_{max}| \geq S_0 \times cos(\phi) + \sigma_{mean} \times sin(\phi) \quad (4)$$

with $\sigma_{mean} = (\sigma_1 + \sigma_3)/2$, $\tau_{max} = (\sigma_1 + \sigma_3)/2$ ($\sigma_1$ and $\sigma_3$ the maximum and minimum principal effective stress respectively), $S_0$ the cohesion of the rock and ϕ the friction angle.

In our model, every point is assumed to be on optimally oriented failure planes in a medium close to failure. Theoretically, in such a medium, even a very small change in the stress state should lead to failure. Hence, the cohesion term ($S_0$) is set to 0MPa. We chose a value of 30° as a plausible friction angle (ϕ) for the TVZ (Kissling et al., 2009).

Theoretically, in a homogeneous medium, the onset of failure would create a plane of weakness, and subsequent failure would preferentially occur along this plane instead of creating new fractures. However, our simple model doesn't consider pre-existing fractures and fracture propagation. We therefore modeled the failure-initiation front propagation through time to gain insights into the possible occurrence and location of failure at each time step, assuming that it had not occurred previously. To a certain extent, this may better represent a natural system that is not uniformly close to failure: Fluids may flow through a part of the medium which is not close to failure, with the induced stresses hence not causing failure. When fluids reach an area close to failure, the associated stress change may lead to failure.

## GENERAL RESULTS

### Stress evolution during the injection

We simulated the evolution of the stresses through time for our reference model. During the first 6 weeks after the start of the injection, the main significant change is the development of a tensile zone very close to the injection zone. Then, this tensile zone becomes surrounded by a compressive zone, itself bound outside by another tensile zone (see Figure 3 after 5 years of injection). Through time, the amplitude of the stresses within these zones increases along with the size of the respective zones. However, most of the changes remain localized within 500 m of the injection zone.

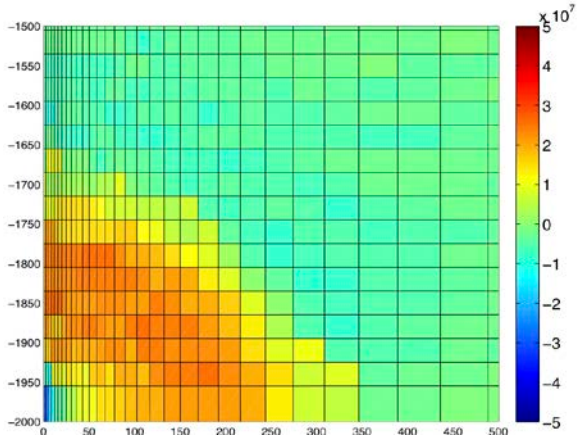


Figure 3. Mean effective stress (Pa) within the domain (axes in meters) after 5 years of injection.

**Poroelastic vs. thermal effect through time**

When studying surface displacement due to the injection of hot fluids into a colder caldera system, Hurwitz et al. (2007) and Hutnak et al. (2009) mentioned that two main processes drive the observed displacement: (1) the poroelastic response (due to increased fluid pressure) and (2) the thermal effect (due to thermal rock expansion). To assess the relative contribution of overpressure and thermal effect to the effective stresses, we ran a range of additional TOUGH2/BIOT2 simulations.

As in Hurwitz et al. (2007), we first assessed exclusively the poroelastic response by inhibiting the thermal effect using a null thermal expansivity coefficient, while the other parameters remained unchanged. Similarly, we then assessed the thermo-elastic response only, by inhibiting poroelasticity using an unrealistic high shear modulus of $5\times10^{11}$GPa. Displacement at each node through time was extracted from each of these simulations, with the associated effective stresses computed using Equations (2) and (3) where G and ν used for the reference model.

In the model where poroelasticity is the dominant effect, some tensile effective stresses appear from the very beginning of the injection and are of high magnitude close to the injection zone (Figure 4). These tensile stresses result from the pore-pressure increase due to fluid flow. However, most of the stress changes for this model remain close to the injection zone during the simulation.

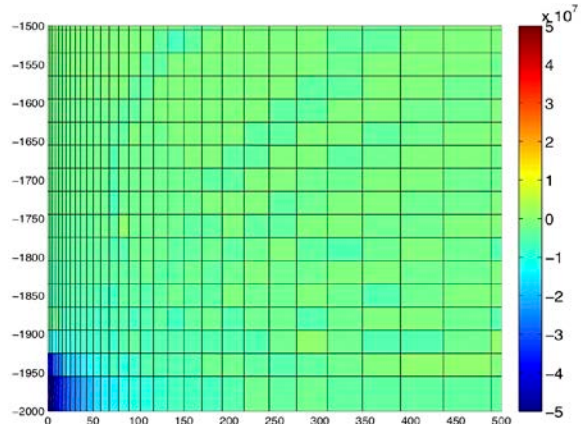


Figure 4. Mean effective stress (Pa) due to poroelastic effect within the domain (axes in meters) after 5 years of injection.

In the model where thermal effect is the main driving process for stress changes, a compressive zone develops close to the injection point, surrounded by a low amplitude tensile zone (Figure 5). These compressive stresses result from the contraction of the rock due to the interaction between cold fluid and hot host rock. Note that these stress changes only become significant after 6 weeks of injection.

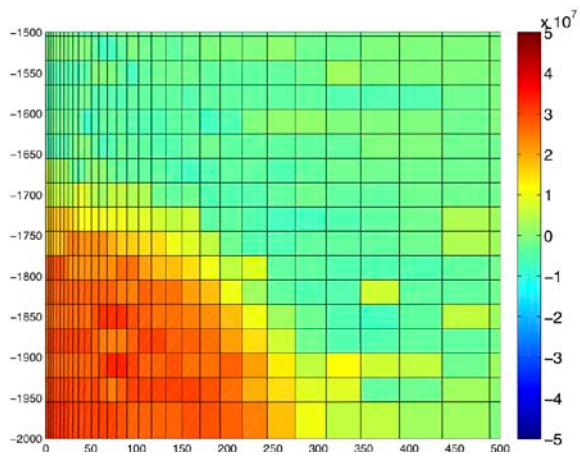


Figure 5. Mean effective stress (Pa) due to thermal effect within the domain (axes in meters) after 5 years of injection.

Then, we compared the results of these simulations with the full poro-thermoelastic reference model to discriminate the main driving process (poroelastic versus thermal) for stress changes through time in the reference model. We observe that the effective stresses for the reference model are the sum of the effective stresses in the poroelastic and thermal models.

Poroelastic effect is then the main process for stress changes at the early stage of the injection. While it remains the main process very close to the injection zone, the thermal effect becomes progressively the dominant effect in the region surrounding this injection zone.

## Failure process

Failure location was simulated through time (Figure 6) using the Mohr-Coulomb criterion defined in Equation (4). We observe that failure occurs from the very beginning of the injection (Figure 6a.). This is expected for a medium close to failure, where even a small change in the stress state can lead to failure. The failure zone is mainly localized within 500 m of the injection point.

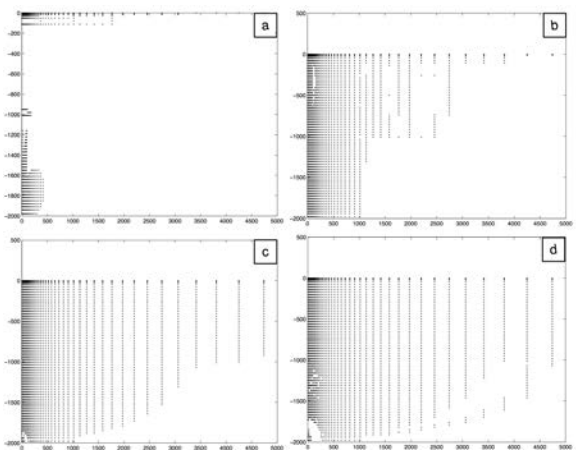


Figure 6. Failure points (black dots) after (a) 1 day (b) 1 month, (c) 1 year, (d) 10 years after the start of the injection (axes in meters).

As mentioned before, if we consider at each time step that there has been no failure at the previous time step, we observe that globally, the size of the potential failure zone increases with time (Figures 6 b., c., d.). Looking more closely at the zone around the injection point, we observe that an aseismic zone develops and becomes wider over time, reaching 300 m radius after 10 years of injection. Moreover, a new seismic zone develops inside this aseismic zone and also increases with time.

We then studied the sign of $|\sigma_{mean_thermo}| - |\sigma_{mean_poro}|$ to assess the dominant process for failure over time. A positive value means that the thermal effect is dominant, whereas a negative value indicates that the poroelastic effect is dominant. At the start of injection, Figure 7 shows that the failure zone coincides with the zone where the mean effective stresses are mainly caused by the poroelastic effect. Thermal stresses also act immediately, but are smaller than those due to poroelastic effect.

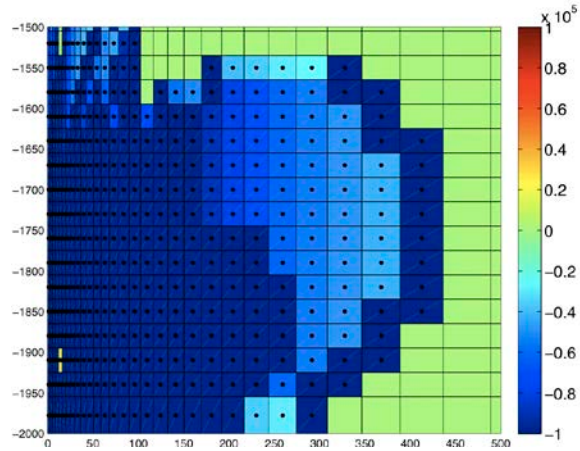


Figure 7. Failure (black dots) and ($|\sigma_{mean_thermo}| - |\sigma_{mean_poro}|$) (colour) after 1 day of injection within the domain (axes in meters).

The aseismic zone developing after a few days of injection clearly coincides with a zone in compression, while the inside seismic zone coincides with a zone in tension (Figure 8). Given these findings, we propose that thermal effect is responsible for the aseismicity while poroelasticity remains the main driver for failure close to the injection zone.

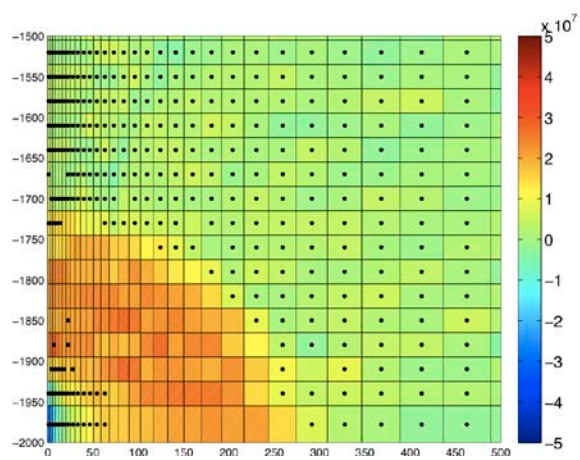


Figure 8. Failure (black dots) and ($|\sigma_{mean_thermo}| - |\sigma_{mean_poro}|$) (colour) after 10 years of injection within the domain (axes in meters).

Finally, the seismic zone around the aseismic zone coincides with a slightly tensile zone, created by both thermal and poroelastic effects.

As a general comment, we note that failure mainly occurs where the stress regime is tensile. This is consistent with the fact that rock is often less resistant in traction than in compression, according to the Griffith criteria, which predicts that the value of the uniaxial compressive strength can be eight or twelve times that of the uniaxial tensile strength (Jaeger et al., 2007).

## SENSITIVITY ANALYSIS

We assessed the effect of key parameters on effective stress changes and failure processes by running additional test simulations. We first considered a medium having a cohesion of 1MPa as used by Kissling et al. (2009) when studying the brittle/ductile transition at the TVZ, then a medium having a friction angle of 45° because it can be representative for andesite (Carmichael, 1982), commonly found at TVZ geothermal fields. We also used end-member shear moduli (1 and 20 GPa) to account for uncertainty in the local velocity models, along with a range of thermal expansivity coefficients ($10^{-6}$ to $10^{-4}$ °$C^{-1}$). Finally, a range of plausible injection rates and temperatures for the injected fluid were used to define the impact of injection parameters. A summary of the various test parameters is presented in Table 2. Note that the shear modulus, thermal expansivity coefficient, injection rate, and temperature of the injected fluid impact both the stress changes and failure process, whereas rock cohesion and friction angle affect the failure process only.

Table 2. Input parameters for TOUGH2/BIOT2 the simulations used for this study sensitivity analysis.

| Parameter | Simulation values |
|---|---|
| Cohesion (MPa) | 0, 1 |
| Friction angle (°) | 30, 45 |
| Shear modulus (MPa) | 1, 8, 20 |
| Therm. exp. coef. (°$C^{-1}$) | $10^{-6}$, $10^{-5}$, $10^{-4}$ |
| Injection rate (t/day) | 100, 225, 350, 475 |
| Inj. fluid temp. (°C) | 135, 140, 145, 150, 155, 160, 165 |

We observe the following points:

- Increasing the rock cohesion does not affect failure within 500 m from the injection zone, but leads to less failure further away.
- Increasing the friction angle has no clear effect on the failure process in the models.
- Increasing the shear modulus (i.e., the rigidity of the medium) decreases the poroelastic effect while not affecting the thermal effect (this was the assumption of our modeling strategy, to account exclusively for the thermal effect) and hence, leads to less failure.
- Increasing the coefficient of thermal expansion increases the thermal effect while not affecting the poroelastic effect, and leads to less failure close to the injection zone.
- Increasing the injection rate increases the poroelastic effect (because of a greater pore pressure) and a wider zone of the model is affected by stress changes. This leads to more failure within the domain.
- Increasing the temperature of the injected fluid does not affect the poroelastic effect but decreases the thermal effect, because the fluid temperature becomes closer to the medium one. However, we do not observe any clear effect on the failure process, possibly due to the limited range of tested temperatures.

To summarize, failure can be minimized by selecting host rock with high cohesion, shear modulus, and thermal expansivity coefficient (thus requiring good knowledge of the pre-injection rock properties) and by using a reasonably low injection rate and an injected fluid temperature close to that of the medium.

## CONCLUSION

We presented results from numerical modeling of fluid flow due to re-injection and its effect on stress changes and failure, in a domain using parameters encountered at a typical TVZ geothermal field. While our models are simplified and do not include, for instance, either fractures or the regional stress field, they still provide insights into the fundamental processes poten-

tially driving induced seismicity. The computed effective stresses show three distinct main zones across the domain: a tensile zone very close to the injection point (1), surrounded by a compressive zone (2), and an external tensile zone (3). These zones change in magnitude and size through time, but most of the changes remain within 500 m of the injection zone.

The effective stresses were computed independently for various effects: poroelastic only, thermal only, and combined poroelastic and thermal. The results show that the effective stresses due to combined poroelastic and thermal effects represent the sum of the individual poroelastic and thermal-related effective stresses. Moreover, the effective stresses due to poroelasticity are tensile, due to the increase in pore pressure, and localized close to the injection area. Conversely, the effective stresses due to thermal effects are mainly compressive, where the temperature decreases due to cold fluid injected into a hot rock, and tensile at the margins of the compressive zone.

Failure -following a Mohr-Coulomb criterion, occurs at the very beginning of the injection within 500 m of the feed zone and is mainly driven by the poroelastic effect. Through time, assuming that there is no propagation of the pre-existing fractures but failure on new fractures, a small seismic zone remains close to the injection zone (with dominant poroelastic tensile stresses). It becomes surrounded by an aseismic zone with dominant compressive thermal stresses, and, further away, by another seismic zone (resulting from poroelastic and thermal tensile stresses).

A sensitivity analysis was performed to assess how the cohesion of the rock, coefficient of internal friction, shear modulus, thermal expansivity coefficient, injection rate, and temperature of the injected fluid impact the effective stress evolution and the failure process. Results suggest that failure can be mitigated by using low injection rates and a fluid temperature close to that of the host rock—or by selecting a site where the medium has high cohesion, shear modulus and thermal expansivity coefficient.

Further modeling work could include:

- Changing the depth of the injection point source to account for stress changes and potential failure below the injection point.
- Fine-tuning our mesh and time stamps to provide more accuracy with respect to location and timing of the observed changes.
- Introducing sinks that represent the production wells.
- Modeling a shut-in in pressure to see the evolution of the poroelastic and thermal effect when re-injection stops. Indeed, there have been several cases in which induced seismicity occurred after the end of the injection.
- Introducing fractures into the model to be more representative of real cases. Along the same lines, some further testing needs to be carried out to consider the effect of permeability, especially since this model uses a relatively low value compared to what could be observed in geothermal fields where fluid flow is fracture-controlled.
- Accounting for the regional stress field.
- Using the two-way TOUGH/FLAC modeling package (Rutqvist et al., 2002) to better account for coupled thermo-hydrological and mechanical processes.

However, even using a simple model, our work shows the fundamentals of what can cause failure and seismicity in active geothermal areas. This study therefore represents a first step towards a more complete assessment of the relative contribution of poroelasticity and thermal effects on induced seismicity.

## ACKNOWLEDGMENT

We are grateful to Shaul Hurwitz and Mike Hutnak (USGS, Menlo Park, USA) for providing us the TOUGH2/BIOT2 simulation codes, and stimulating discussions. We also thank Mighty River Power, particularly Steven Sewell for discussions on the Rotokawa geothermal field. This project was initially funded by Foundation for Research Science and Technology “Geothermal: New Zealand's Energy Solution,” which has (from 1 July, 2011)

been incorporated into the GNS Science CSA (Core Science Area) Geothermal Research. Finally, we thank Patrick Baud and Francois Cornet for early reviews of this work.

## REFERENCES

Bowyer D, and R. Holt, Case Study: Development of a numerical model by a multi-disciplinary approach, Rotokawa Geothermal Field, New Zealand, *Proceeding World Geothermal Congress 2010, Bali Indonesia, 25-29 April 2010*, 2010.

Carmichael, R., *Handbook of Physical Properties of Rocks*, CRC Press, 1982.

Hsieh, P.A., Deformation-induced changes in hydraulic head during ground-water withdrawal, *Ground Water, 34*, 1082-1089, 1996.

Hurwitz, S., L. B. Christiansen and P. A. Hsieh, Hydrothermal fluid flow and deformation in large calderas: Inferences from numerical simulation, *J. Geophys. Res., 112*, B02206, doi:10.1029/2006JB004689, 2007.

Hutnak, M., S. Hurwitz, S. E. Ingebritsen, and P. A. Hsieh, Numerical models of caldera deformation: Effects of multiphase and multicomponent hydrothermal fluid flow, *J. Geophys. Res., 114*, B04411, doi:10.1029/2008JB006151, 2009.

Jaeger, J., N. Cook, and R. Zimmerman, *Fundamentals of Rock Mechanics* (4th ed), Blackwell Publishing, 2007.

Kissling, W., S. Ellis, F. Charpentier, and H. Bibby, Convective flowa in a TVZ-like setting with a brittle/ductile transition, *Transport in Porous Media, 77*, 335-355, 2009.

Majer, E., R. Baria, M. Stark, S. Oates, J. Bommer, B. Smith, and H. Asanuma, Induced seismicity associated with enhanced geothermal systems, *Geothermics, 36(3)*, 185-222, 2007.

Pruess, K., C. Oldenburg, and G. Moridis, *TOUGH2 User's Guide, Version 2.0*, Report LBNL-43134, Lawrence Berkeley National Laboratory, Berkeley, Calif., 1999.

Rutqvist, J., Y. S. Wu, C-F Tsang, and G. Bodvarsson, A modeling approach for analysis of coupled multiphase fluid flow, heat transfer, and deformation in fractured porous rock, Int. J. Rock Mech. Min. Sci., 39,429-442, doi:10.1016/j.ijrmms.2007.04.006, 2002.